EurJIC
European Journal of Inorganic Chemistry

A Journal of ChemPubSoc Europe

Accepted Article

Title: Crystal Structures and Spin-Crossover Behavior of Iron(II) Complexes with Chiral and Racemic Ligands

Authors: Yusuke Sekimoto, Mohammad Razaul Karim, Naoto Saigo, Ryo Ohtani, Masaaki Nakamura, and Shinya Hayami

To be cited as: *Eur. J. Inorg. Chem.* 10.1002/ejic.201601232

Link to VoR: http://dx.doi.org/10.1002/ejic.201601232

WILEY-VCH

Crystal Structures and Spin-Crossover Behavior of Iron(II) Complexes with Chiral and Racemic Ligands

Yusuke Sekimoto,[a] Mohammad Razaul Karim,[a,b] Naoto Saigo,[a] Ryo Ohtani,[a] Masaaki Nakamura,[a] Shinya Hayami*[a,c]

Abstract: Chiral and racemic iron(II) complexes, [Fe((*R*)-L)$_2$(NCS)$_2$] (**1**), [Fe((*S*)-L)$_2$(NCS)$_2$] (**2**) and [Fe(*R*,*S*)-L)$_2$(NCS)$_2$] (**3**) (L = α-methyl-*N*-(2-pyridinylmethylene)-cyclohexanemethanamine) were synthesized. Their structures and the magnetic properties were investigated by the X-ray analysis, the magnetic susceptibility and Mössbauer spectra measurements. Complexes **1** and **2** were crystallized in trigonal system with space groups *P3$_1$21* and *P3$_2$21*, respectively. All complexes exhibited spin-crossover (SCO) behaviors and light induced exited spin state trapping (LIESST) effects at 532 nm. Complexes **1** and **2** showed similar gradual SCO behavior and complex **3** more gradual SCO, which seems to be different crystal molecular packing, since complex **3** is the symmetric isomer, and **1** and **2** are asymmetric.

Introduction

In recent years, chiral magnetic systems are increasingly attracting attention in the prospects of magneto-optical devices, chiral magnetism, and chiral catalysis.[1] Enantiopure magnetic materials based on the interactions between pendant chiral groups and macrocyclic metal complexes have been reported.[2] The expected magnetic property in terms of SCO phenomenon involves external perturbations (*e.g.*, temperature, pressure, magnetic field or light) from induced transition between low spin (LS) and high spin (HS) states in the solid phase of the first transition metal complexes with $3d^n$ (n = 4-7) electronic configurations.[3] Iron(II) SCO complexes, [Fe(L)$_2$(NCX)$_2$] (L = bidentate or tetradendtate ligand; X = S or Se), have been extensively studied as the SCO behaviors are affected according to their stereoisomerism (*cis*/*trans* or *mer*/*fac*) of the coordinated polydentate and NCX ligands. Interestingly, only *cis* isomer between *cis*- and *trans*-[Fe^{II}(triaryltriazole)(NCS) complexes showed SCO behavior.[4] Matouzenko *et al*. have reported the abrupt SCO behavior in [Fe(DPEA)(NCS)$_2$] (DPEA = (2-aminoethyl)*bis*(2-pyridyl-methyl)-amine)), where the tetradentate ligand (DPEA) and NCS$^-$ are in *mer* and *cis* position, respectively.[5] Its cooperativity was triggered by numerous intermolecular interactions including hydrogen-bonding and van der Waals forces throughout neighboring molecules. Optically active complexes, either Δ- and Λ-isomer, much drew attention to magnetic properties. Boinnard *et al.* have suggested from the different average bond length of racemic-[Fe^{II}(5-NO$_2$-sal-N(1,4,7,10))] complex that the iron(II) of Λ-isomer was low-spin but the iron(II) of the Δ-isomer was high-spin.[6] In the intermediate phase of its two step spin transition phenomenon, half of the molecules are associated with both *S* = 0 (Λ enantiomer) and *S* = 2 (Δ enantiomer) states. Homochiral SCO complexes generated by spontaneous resolution have been also reported.[7] For the effect of Δ/Λ configuration on SCO behavior, optically active and racemic metal complexes, [Fe((*R*)-L)$_2$(NCS)$_2$] (**1**), [Fe((S)-L)$_2$(NCS)$_2$] (**2**) and [Fe((*rac*)-L)$_2$(NCS)$_2$] (**3**) (L = α-Methyl-*N*-(2-pyridinylmethylene)-cyclohexanemethanamine), were prepared[8], respectively and characterized by powder XRD, X-ray crystallography, and Mössbauer spectra.

Results and Discussion

The crystal data and structural details are summarized in Table S1.[9,10] ORTEP drawings for **1** and **2** are shown in figure 1. The complex **2** was crystallized in the chiral space group *P3$_2$21*. The molecular symmetry of the complexes could not affirm due to the chirality of ligands and complexes and the general features of the structures as previous report.[11] Each iron atom is octahedrally coordinated with four nitrogen atoms of two chiral bidentate ligands and two thiocyanato ions arranged by cis configurarion. The bond lengths of Fe-N at 278 K match with typical values for HS iron(II) species. The two Fe-N(pyridine) distances, Fe-N(1) and Fe-N(2), are 2.188(4) and 2.195(4) Å, respectively. The Fe-N(imine) distances (Fe-N(3) = 2.292(4) and Fe-N(4) = 2.240(7) Å) are longer than Fe-N(pyridine). The Fe-N(CS) distances (Fe-N(5) = 2.129(6) and Fe-N(6) = 2.072(9) Å) are shorter than other Fe-N(pyridine and imine). The steric hindrance was reflected in N-Fe-N angles. The N-Fe-N bond angles between adjacent and opposite nitrogen atoms are within the range of 74.6(2)° to 99.01(17)° and 166.2(2)° to 167.1(2)°, respectively (Table S1). The less differences in bond lengths and angles of complex **2** imply more regulated octahedral geometry as compared with analogues, [Fe(PM-BiA)$_2$(NCS)$_2$] (PM is *N*-2-pyridylmethylene and BiA is 4-aminobiphenyl).[12] All molecules of **2** consist of Λ-enantiomer in the single crystal and are consistent with Flack parameter. Optically active Δ or Λ complex can be introduced by the chiralirty or steric hinderance

---

[a] Department of Chemistry, GSST, Kumamoto University,
2-39-1, Kurokami, Chuo-ku, Kumamoto860-8555, Japan
E-mail:hayami@sci.kumamoto-u.ac.jp
[b] Department of Chemistry, School of Physical Sciences, Shahjalal
University of Science & Technology, Sylhet-3114, Bangladesh
[c] Institute of Pulsed Power Science (IPPS), Kumamoto University,
2-39-1, Kurokami, Chuo-ku, Kumamoto860-8555, Japan
E-mail: hayami@sci.kumamoto-u.ac.jp

Supporting information for this article is given via a link at the end of the document.((Please delete this text if not appropriate)) of the coordinating ligands.[11] Supposed that two cyclohexyl groups are orientated parallel to another ligands for proper intermolecular packing in the single crystals. Any H-bonding or *π*-*π* interaction was not found in the crystal structure. Van der Waals interaction was also formed between **2** in this crystal packing. Structure **1** is almost same as **2** except different absolute configuration. The single crystal **3** was analyzed by X-ray crystallography but the cyclohexyl moiety were highly disordered and the *R* value was not improved. The powder X-ray diffraction (PXRD) pattern of **3** is well matched by the simulated one from the single crystal (Figure. S1).

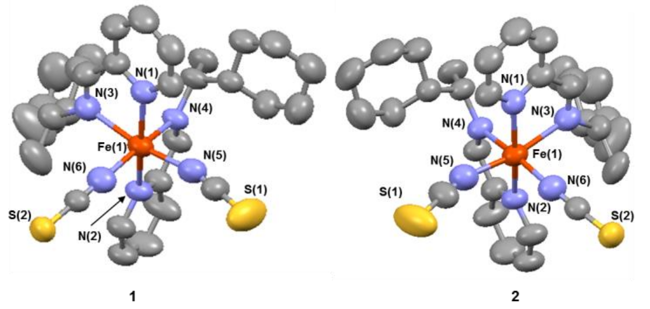

Figure 1. Single crystal structures of **1** and **2** at 298 and 278 K, respectively. Hydrogen atoms are omitted for clarity; thermal ellipsoids are at the 50% probability level.

The magnetic properties of **1**, **2** and **3** were measured in the temperature range of 5 to 400 K (Figure 2), whereas Mössbauer spectra were obtained at 80 and 295 K (Figure S3, S5, S6, S8 and Table S3-S5). The magnetic susceptibilities are shown in Figure 2 after removing the solvents by annealing under vacuum condition. The $\chi_M T$ values of **2** with 2.82 cm^3 K mol^{-1} above 310 K resembles with HS iron(II) complexes. On cooling mode, the $\chi_M T$ value was gradually decreased, exhibiting incomplete SCO behaviour ($T_{1/2}$=230 K). The $\chi_M T$ value at 80 K with 1.62 cm^3 K mol^{-1} implies 58 % of HS fraction. Since the decrease of $\chi_M T$ value below 30 K corresponds to zero-field splitting, this is not two-step SCO behavior. The plateau behavior is caused by the mixture of HS and LS domains.

The Mössbauer spectra match with the magnetic behavior. The Mössbauer spectrum of **2** at 295 K consists of one doublet as the main peak (Figure S5). The isomer shift (I.S.) of the doublet and the quadruple splitting (Q.S.) as 0.99 and 2.34 mms^{-}, respectively, are typical appearance for the HS state of iron(II).[1] Two kinds of doublet including wide (I.S. = 1.16 mms^{-1}, Q.S. = 3.10 mms^{-1}) and narrow (I.S. = 0.49 mms^{-1}, Q.S. = 0.56 mms^{-1}) doublet at 80 K are assigned to the HS and LS state of iron(II) species, respectively. The ratio of HS species (estimated form area ratio) in **2** was 41 %. **2** exhibited the LIESST effect, as well (Figure S4). Irradiation with laser (532 nm) at 5 K afforded the increasement in $\chi_M T$ value from 0.92 to 1.38 cm^3 K mol^{-1}, which is implicative for the trapping of metastable HS state. When the light was switched off, $\chi_M T$ value increased to 1.87 cm^3 K mol^{-1} at 40 K on warming mode. The $\chi_M T$ value within 40 to 70 K range was decreased by HS → LS thermal relaxation (T_{LIESST} = 60 K), and recovered to the original one above 70 K.

Despite the XRD data for **2** at 110 K, the *R* value (= 11.43) was not improved but we estimated all Fe-N distances. There are two units in the crystal packing of **2** at 110 K and the all Fe-N bonds are shown in Table S2. The average bond lengths of Fe-N are almost same in each unit, one is 2.121(6) and the other 2.132(2) Å. Therefore, HS and LS states do not coexist in the crystals, which suggest the HS-LS stabilization in the packing at low temperature does not come from a mixture of HS and LS states but a mixture of HS and LS domains in microstructural scale. Compared the XRD data for **2** between HS and LS state, most of Fe-N bonds were decreased when HS state was transformed to LS state. The Fe-N distances of **2** range from 2.072(9) to 2.292(4) Å in the HS state and from 2.05(1) to 2.20(1) Å in LS state. Compared with the case of Marchivie and coworkers,[12] these decline are not enough to exhibit abrupt SCO behavior. Furthermore, one of Fe-N(NCS) bonds at 110 K is 2.12(1) Å and longer than 2.072(9) Å at 278 K, which explain why **1** and **2** exhibit gradual and incomplete spin crossover behavior.

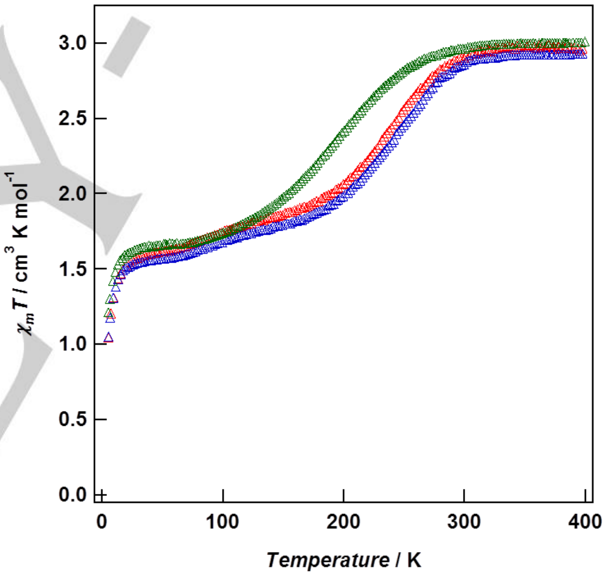

Figure 2. Temperature dependence of magnetic susceptibilities ($\chi_m T$) for the single crystals of **1** (△), **2** (△) and **3** (△).

Being enantiomeric pair **1** and **2** possess almost similar crystal structures (except the configurations of the coordinated ligands and complexes), the magnetic behavior of **1** is similar to **2**. The $\chi_M T$ value of the compound **1** at higher than 310 K was ca. 2.94 cm^3 K mol^{-1} and 1.68 cm^3 K mol^{-1} at 80 K (Figure S2). The $\chi_M T$ value at 80 K corresponds to 57 % of HS fraction and $T_{1/2}$ is 230 K. The Mössbauer spectra of the compound **2** showed one doublet (I.S. = 1.00 mms^{-1}, Q.S. = 2.31 mms^{-1}) at 295 K, the wide doublet (I.S. = 1.16 mms^{-1}, Q.S. = 3.09 mms^{-1}) at 80 K and narrow doublet (I.S. = 0.48 mms^{-1}, Q.S. = 0.54 mms^{-1}) at 80 K. And the HS fraction was 45 % (Figure S3 and Table S3). For the compound **1**, the LIESST effect was observed as well as the compound **2**, of which T_{LIESST} was 60 K.

The powdered compound **3** exhibited different magnetic behavior comparing the compounds **1** and **2**. The spin state at 400 K was expected to nearly HS state with the $\chi_M T$ value of 2.99 cm^3 K mol^{-1}. On cooling, the $\chi_M T$ value showed more noticeable decrease ($T_{1/2}$ = 214 K) than that of the compounds **1** and **2**. The $\chi_M T$ vs. T curve became plateau at 30 to 80 K and the $\chi_M T$ value was 0.90 cm^3 K mol^{-1}, which corresponds to 30 % of HS fraction. The Mössbauer parameters indicated that iron(II) at 295 K was nearly HS state (I.S. = 1.01 mms^{-1}, Q.S. = 2.39 mms^{-1}), and the one at 80 K coexisted in HS (I.S. = 1.07 mms^{-1}, Q.S. = 3.00 mms^{-1}) and LS state (I.S. = 0.43 mms^{-1}, Q.S. = 0.57 mms^{-1}). The ratio of the HS fraction was 23 % at 80 K. The noticeable spin conversion at low temperature was detected by Mössbauer spectrum and magnetic susceptibilities for powdered sample of the compound **3**, which also exhibited the LIESST effect. The $\chi_M T$ value was increased from 0.44 cm^3 K mol^{-1} to 0.74 cm^3 K mol^{-1} by laser irradiation at 5 K and showed maximum value (1.15 cm^3 K mol^{-1}) at 40 K as 11% of LS → HS spin conversion. The thermal relaxation was back to the original state at above 70 K (T_{LIESST} = 60 K). By comparison these values with the ones of solvent-free complexes, the dissimilarity between **2** (or **1**) and **3** is not derived from the solvent nature.

From spin crossover behavior between single crystal and powder sample of the compound **3**, the $\chi_M T$ value of single crystals was ca. 2.70 cm^3 K mol^{-1} at above 310 K and 1.40 cm^3 K mol^{-1} at 80 K (Figure 2). These values are close to the compounds **1** and **2** rather than powder sample of **3**. The HS fraction at 80 K was estimated 53 % from $\chi_M T$ value. The $T_{1/2}$ for single crystal of **3** (193 K), however, was different from the ones for compounds **1** and **2** (230 K). The Mössbauer spectrum for single crystal of the compound **3** at 295 K showed only one doublet (I.S. = 0.99 mms^{-1}, Q.S. = 2.38 mms^{-1}), which is assigned to HS species of iron(II) as well as other samples (Figure S6 and Table S4). Its spectrum at 80 K reflects magnetic susceptibility data and consists of the wide doublet (I.S. = 1.11 mms^{-1}, Q.S. = 3.12 mms^{-1}) and narrow doublet (I.S. = 0.43 mms^{-1}, Q.S. = 0.58 mms^{-1}). The HS fraction at 80 K obtained from area ratio was 45 %.

Mössbauer fitting parameters for mixture of **1** and **2** at 80 K are summerized in Table 1. Since the preparative condition of each sample such as stirring time or amount of solvent was not the same, percentage of HS and LS fraction in the complex is not expected to follow the R:S ratio of the ligand. However, the addition of one enantiomer to a homogeneous racemic mixture (50:50 for R:S) may promote more spin conversion and this effect is mainly likely because of the crystal defects. The SC behavior is influenced by the preparative procedure or additional post-preparative treatment such as ball-milling or crushing in a mortar.[13] These effects are mainly caused by crystal defects. However, such crystal defects increases residual HS fraction and/or results in less steep spin transition curve. The powder samples are regarded having more crystal defects than single crystal. However, HS → LS spin conversion is promoted at low temperature in the powder sample of **3** (Figure S6, S8, Table S4 and S5). To the best of our knowledge, such example has not been reported so far. In case of pure single crystal, i.e. HS:LS = 50:50, of compound **3** at low temperature, it should be stabilized by····HS-LS-HS-LS···· assembly as the reported phenomenon for 2 step SCO behaviour of [Fe(2-pic)$_3$]Cl$_2$·EtOH (2-pic = 2-picoline or 2-aminomethylpyridine) or dinuclear complexes.[14] We assume (the data sequence in Table 2 also imply) that even in **1** and **2**, establishment of ····HS-LS-HS-LS···· type stabilization at low temperature through the spin conversion to LS species is possible by mixing *R* and *S* enantiomer, respectively. Such effect was observed by adding 10% of the opponent enantiomer. Therefore, single crystals of **1**, **2** and **3** are stabilized as ····HS-LS-HS-LS···· formation at low temperature. Depending on the extent of chirality, the crystal structures affect cooperativity, which results in the difference in $T_{1/2}$ value. A packing preference for ····HS-LS-HS-LS···· stabilization seems that such patterning is naturally favoured to afflict the anisotropy of molecules caused by chirality and distortion. Array of chiral molecules in the crystals might render stabilizing factors such as dipole-dipole interactions then the····HS-LS-HS-LS···· type formation recover the loss in stabilization.

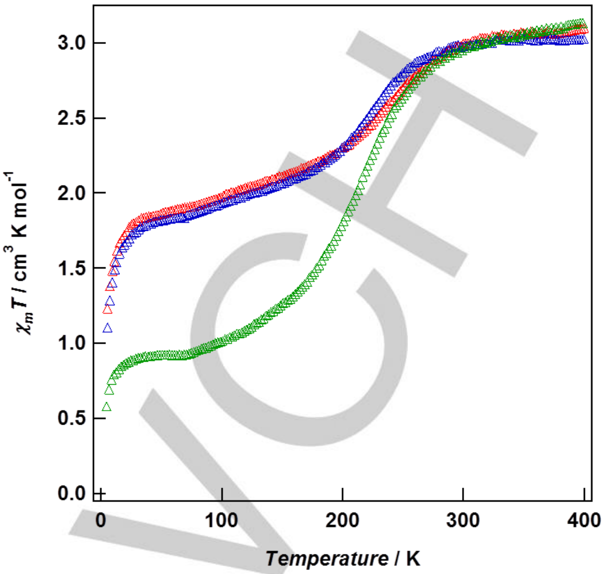

Figure 3. Temperature dependence of magnetic susceptibilities ($\chi_m T$) for the powder samples of **1** (△), **2** (△) and **3** (△)

Table 1. Mössbauer fitting parameters for mixture of **1** and **2** at 80 K.

R:S		I.S. (mm s^{-1})	Q.S. (mm s^{-1})	Γ (mm s^{-1})		Area ratio (%)
100:0	HS (Fe^{II})	1.16	3.09	0.36	0.37	45.3
	LS (Fe^{II})	0.48	0.54	0.37	0.38	54.7
90:10	HS (Fe^{II})	1.07	3.04	0.31	0.33	21.2
	LS (Fe^{II})	0.41	0.55	0.32	0.32	78.8
80:20	HS (Fe^{II})	1.08	3.03	0.32	0.31	28.0
	LS (Fe^{II})	0.42	0.55	0.32	0.31	72.0
70:30	HS (Fe^{II})	1.08	3.03	0.30	0.36	22.4
	LS (Fe^{II})	0.42	0.56	0.30	0.30	77.6
60:40	HS (Fe^{II})	1.08	3.02	0.34	0.37	28.6
	LS (Fe^{II})	0.42	0.56	0.36	0.34	71.4
50:50	HS (Fe^{II})	1.07	3.00	0.35	0.49	22.6
	LS (Fe^{II})	0.43	0.57	0.41	0.36	77.4
40:60	HS (Fe^{II})	1.08	3.01	0.33	0.38	27.6
	LS (Fe^{II})	0.42	0.56	0.35	0.33	72.4
30:70	HS (Fe^{II})	1.07	3.04	0.31	0.35	29.4
	LS (Fe^{II})	0.41	0.56	0.35	0.33	70.6
20:80	HS (Fe^{II})	1.08	3.03	0.32	0.34	25.7
	LS (Fe^{II})	0.41	0.56	0.35	0.34	74.3
10:90	HS (Fe^{II})	1.07	3.07	0.31	0.35	24.1
	LS (Fe^{II})	0.41	0.56	0.37	0.35	75.9
0:100	HS (Fe^{II})	1.16	3.10	0.34	0.33	41.3
	LS (Fe^{II})	0.49	0.56	0.38	0.34	58.7

Conclusions

[Fe((*R*)-L)$_2$(NCS)$_2$] (1), [Fe((*S*)-L)$_2$(NCS)$_2$] (2), and [Fe((*rac*)-L)$_2$(NCS)$_2$] (3) were prepared by using chiral/racemic ligands as the starting materials. 1 and 2 existed in *Δ* and *Λ* enantiomer, respectively. All complexes exhibited SCO behavior. The SCO behaviors for 1 and 2 showed no differences in their magnetic property but 3 was different from the one of 1 and 2. The $T_{1/2}$ value for 3 at 230 K and for 1 and 2 at 204 K displayed such variation. The racemic complex which was prepared by 50:50 ratio of each enantiomeric ligand existed as major contribution of HS state. But an increased chirality (prepared from higher ratio of either *R* or *S*) resulted in an increasing contribution of the LS state.

Experimental Section

(*R*,*S*)-*N*-(1-cyclohexylethyl)-1-(pyridin-2-yl)methanimine

(*R*)-, (*S*)-, and (*R,S*)-*N*-(1-cyclohexylethyl)-1-(pyridin-2-yl)methanimine (L): (*R*)-, (*S*)-, or (*R,S*)-Cyclohexylethylamine (0.25 g, 2.0 mmol) and pyridine-2-carboxyaldehyde (0.21 g, 2.0 mmol) were stirred in methanol (20 mL) for 3 h. Removal of solvent under reduced pressure gave yellow oil. The product was of high purity and used next steps without further purification. ^{1}H NMR (400MHz) in CDCl$_3$: δ 0.8-2.0 (m), 3.44 (s, 1H), 3.12 (m, 1H), 7.28 (t, 1H), 7.70 (t, 1H), 8.04 (d, 1H), 8.61 (d, 1H).

[Fe((*R*)-L)$_2$(NCS)$_2$] (1), [Fe((*S*)-L)$_2$(NCS)$_2$] (2), and [Fe ((*rac*)-L)$_2$(NCS)$_2$] (3): FeCl$_2$·4H$_2$O (0.20 g, 1.0 mmol)~~,~~ was dissolved in methanol (5 mL) in the presence of a small amount of ascorbic acid to prevent oxidation of iron(II). KSCN (0.19 g, 1.0 mmol) in methanol (5 mL) was added and the mixture stirred for 15 minutes. The solution was separated from white precipitate of potassium chloride by filtration and added dropwise to the ligand, **L** (2 mmol) with stirring in deoxygenated methanol (20 mL). The color of solution turned to violet and the precipitate was formed immediately. The solid was filtered, washed with a small amount of cold methanol and dried under vacuum. Yield: 0.39 g (62.9%). Element. Anal. Calcd. for $C_{31}H_{44}Fe_1N_6O_1S_2$: C, 58.84; H, 6.97; N, 13.20. Found: C, 58.72; H, 6.74; N, 13.34 %. IR: v_{max}/cm^{-1}; 2925, 2852 (v_{CH}), 2076, 2063 (v_{CN}) (KBr). The single crystal was obtained from diffusion of diethylether into a chloroform solution of each complex. **1** and **2** were prepared by using either (*R*)-**L** or (*S*)-**L**, respectively. **3** was prepared by using 1:1 mixture of of (*R*)-**L** and (*S*)-**L**.

Physical measurement: The structure of the compounds **1** and **2** were determined at 298 K and 278K, respectively. The crystals mounted on a glass capillary. All the measurements were made on a Rigaku/MSC Mercury CCD diffractometer with graphite monochromated Mo-K*α* (*λ*= 0.71070 Å) radiation. The data were collected at 298±2 K and 278±2 K, respectively. The maximum 2*θ* value is 55.0º. A total of 1240 oscillation images were collected. Data were collected and processed using the Crystalclear program (Rigaku). The linear absorption coefficients, *μ*, for Mo-K*α* radiation were 5.55 cm^{-1}, 5.57 cm^{-1}, respectively. The data were corrected for Lorentz and polarization effects. The structure was solved by direct method (SIR-92) and expanded using Fourier techniques. The non-hydrogen atoms were refined anisotropically. Hydrogen atoms were included for structure analysis but not refined. The final cycle of full-matrix least-squares refinement was based on all reflections. Computations were carried out on a SGI O2 computer using teXsan crystallographic software package. The magnetic susceptibilities *χ*(*T*) were measured between 5 K and 400 K with a superconducting quantum interference device magnetometer (Quantum Design MPMS-5S) in an external field of 0.5 T. LIESST experiment was done with using an Ar$^+$ laser (*λ* = 532 nm, continuous wave) as a light source. The Mössbauer spectrometer, with a ^{57}Co/Rh source, was driven in the transmission mode.

Keywords: Iron(II) compound • Chirality • Stereochemistry • Spin crossover • Mössbauer spectra

[1] a) M. Mito, K. Iriguchi, H. Deguchi, J. Kishine, K. Kikuchi, H. Ohsumi, Y. Yoshida and K. Inoue, *Phys. Rev. B*, **2009**, *79*, 012406/1-012406/4. b) C. Train, R. Gheorghe, V. Krstic, L. M. Chamoreau, N. S. Ovanesyan, G. L Rikken, M. Gruselle, M. Verdaguer, *Nat. Mater*, **2008**, *7*, 729-734. c) J.-M. Lehn, *Supramolecular chemistry, Concept and Perspectives*, Wiley-VCH, Weinheim, **1995**.

[2] a) S. Yamamura, Y. Sugawara, K. Suzuki, T. Sugawara, *J. Am. Chem. Soc.*, **2010**, *132*, 4528-4529. b) M. Kurmoo, A. W. Graham, P. Day, S. J Coles, M. B. Hursthouse, J. L. caufield, J. Singleton, F. L. Pratt, W. Hayes, L. Ducasse, P. Guionneau, *J. Amer. Chem. Soc.*, **1995**,*117*, 12209-12217. c) H.-R. Wen, C.-F. Wang, Y. Song, J.-L. Zuo, X.-Z. You, *Inorg. Chem.*, **2005**, *44*, 9039-9045. d) J. H. Han, M. J. Cha, B. G. Kim, S. K. Kim, K. S. Min, *Inorg. Chem. Commun.*, **2008**, *11*, 745-748.

[3] a) J. Olguín, S. Brooker, *Coord. Chem. Rev.*, **2011**, *255*, 203-240. b) Y. Garcia, F. Robert, A. D. Naik, G. Y. Zhou, B. Tinant, K. Robeyns, S. Michotte, L. Piraux, *J. Am. Chem. Soc.*, **2011**, *133*, 15850-15853. c) X.-Y. Wang, C. Avendaño, K.R. Dunbar, *Chem. Soc. Rev.*, **2011**, *40*, 3213-3238.

[4] D. Zhu, Y. Xu, Z. Yu, Z. Guo, H. Sang, T. Liu, X. You, *Chem. Mater.* **2002,** *14,* 838-843.

[5] G. S. Matouzenko, A. Bousseksou, S. Lecocq, P. J. van Koningsbruggen, M. Perrin, O. Kahn, A. Collet, *Inorg. Chem.*, **1997**, *36*, 2975-2981.

[6] D. Boinnard, A. Bousseksou, A. Dworkin, J.-M. Savariault, F. Varret, J.-P. Tuchagues, *Inorg. Chem.*, **1994**, *33*, 271-281.

[7] Y. Sunatsuki, Y. Ikuta, N. Matsumoto, H. Ohta, M. Kojima, S. Iijima, S.Hayami, Y. Maeda, S. Kaizaki, F. Dahan, J. P. Tuchagues, *Angew. Chem. Int. Ed.*, **2003**, *42*, 1614-1618.

[8] a) X.-L. Tong, T.-L. Hu, J.-P Zhao, Y.-K Wang, H. Zhang, X.-stH. Bu, *Chem. Commun.*, **2010**, *46*, 8543-8545. b) A.-K. Klehe, V. Laukhin, P. A. Goddard, J. A. Symington, J. Aghassi, J. Singleton, E. Coronado, J. R. Galan-Mascaros, C. J. Gomez-Garcia, C. Gumez-Garcia, *Synth. Met.*, **2003**, *133*, 549-551.

[9] X-ray crystallographic data for **1** ($C_{30}H_{40}FeN_6S_2$) at 298 K: FW= 604.65, trigonal, space group $P3_121$, a (or b) = 16.6877(4) Å, c = 22.8415(5) Å, V = 5508.69 Å^3, Z = 6, D_{calcd} = 1.094 g cm^{-3}, Flack parameter = 0.00(3), R = 0.0656 for all data with a linear absorption coefficient Mo-Kα radiation = 5.55 cm^{-1}. CCDC 1508831.

[10] X-ray crystallographic data for **2** ($C_{30}H_{40}FeN_6S_2$) at 278 K: FW= 604.65, trigonal, space group $P3_221$, a (or b) = 16.7528(7) Å, c = 22.8703(9) Å, V = 5558.75 Å^3, Z = 6, D_{calcd} = 1.084 g cm^{-3}, Flack parameter = 0.00(2), R = 0.0848 for all data with a linear absorption coefficient Mo-Kα radiation = 5.57 cm^{-1}. CCDC 1508832.

[11] E. Coronado, F. Palacio, J. Veciana, *Angew. Chem. Int. Ed.*, **2003**, *42*, 2570-2572.

[12] a) M. Marchivie, P. Guionneau, J.-F. Létard, D. Chasseau, *Acta Cryst. B*, **2003**, *59*, 479-486. b) P. Guionneau, Dalton Trans., **2014**, 43, 382-393.

[13] a) E. W. Müller, H. Spiering, P. Gütlich, *Chem. Phys. Lett.* **1982,** *93,* 567-571. b) E. W. Müller, H. Spiering, P. Gütlich, *Inorg. Chem.* **1984,** *23,* 119-120.

[14] P. Gütlich, Y. Garcia, T. Woike, *Coord. Chem. Rev.*, **2001**, *219-221*, 839-879

Entry for the Table of Contents (Please choose one layout)

Layout 1:

FULL PAPER

Text for Table of Contents

Chiral [Fe((*R*)-**L**)$_2$(NCS)$_2$] and [Fe((*S*)-**L**)$_2$(NCS)$_2$] (**2**) and racemic [Fe((*rac*)-**L**)$_2$(NCS)$_2$] complexes, where (**L** = *N*-(1-cyclohexylethyl)-1-(pyridin-2-yl)methanimine) exhibited spin-crossover (SCO) behaviors and light induced exited spin state trapping effects

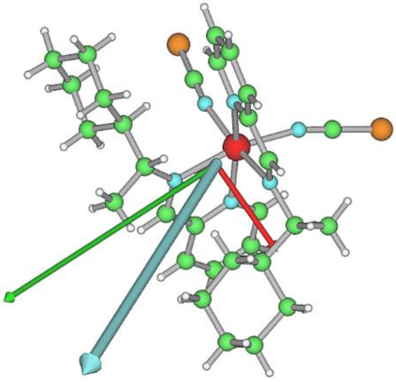

Key Topic*

Chiral Spin-Crossover

*Yusuke Sekimoto, Mohammad Razaul Karim, Naoto Saigo, Ryo Ohtani, Masaaki Nakamura, Shinya Hayami**

*Author(s), Corresponding Author(s)**

Page No. – Page No.

Title

Crystal Structures and Spin-Crossover Behavior of Iron(II) Complexes with Chiral and Racemic Ligands

* Chiral ligand, Spin crossover